Lab on a Chip

Cite this: *Lab Chip*, 2012, **12**, 3111–3116

www.rsc.org/loc

PAPER

Controlled synthesis of fluorescent silica nanoparticles inside microfluidic droplets†

Josias B. Wacker,* Ioannis Lignos, Virendra K. Parashar and Martin A. M. Gijs

Received 28th March 2012, Accepted 22nd May 2012
DOI: 10.1039/c2lc40300e

We study the droplet-based synthesis of fluorescent silica nanoparticles (50–350 nm size) in a microfluidic chip. Fluorescein-isothiocyanate (FITC) dye is first chemically linked to aminopropyl triethoxysilane (APTES) in ethanol and this reaction product is subsequently mixed with tetraethyl orthosilicate (TEOS) to yield a fluorescent silicon alkoxide precursor solution. The latter reacts with an aqueous ethanol–ammonia hydrolysing mixture inside droplets, forming fluorescent silica nanoparticles. The droplets are obtained by pinching-off side-by-side flowing streams of alkoxide solution/hydrolysing mixture on a microfluidic chip using a Fluorinert oil continuous phase flow. Synthesis in droplets leads to a faster reaction and allows drastically improved nanoparticle size uniformity (down to 3% relative standard deviation for 350 nm size particles) when compared to conventional bulk synthesis methods, thanks to the precise control of reagent concentrations and reaction times offered by the microfluidic format. Incorporating FITC inside silica nanoparticles using our method leads to reduced dye leakage and increases the dye's stability, as evidenced by a reduced photochemical bleaching compared to a pure FITC solution.

Introduction

Nanoparticles play an important role in a wide field of applications. They are used in drug delivery,[1] in nano-optical and nano-electrical devices,[2] and as fluorescent biosensors,[3] to name only a few. Many of these applications rely on physico-chemical phenomena that are tightly linked to the size of the nanoparticles and involve the use of microdevices.[4,5] Traditionally, nanoparticles are synthesized in large quantities and in a batch-wise manner. However, using these procedures, controlling their size and size distribution is not straightforward.[6,7] Additionally, the mismatch in produced quantities and the ultimately used number of particles in microdevices often results in an excess of products and the waste of reagents.

In their seminal work, Khan *et al.* used the concept of segmented flow and synthesized silica nanoparticles in microfluidic chips by compartmentalizing a continuous flow of liquid reagents with air, thus creating microreactors (slugs) with a volume of a few nL.[8] However, in gas–liquid segmented flows, the liquid phase may form a film on the channel walls through which reagents and nanoparticles can be exchanged between single compartments, which may broaden the particle size distribution. A better chemical isolation of the compartments can be achieved by replacing the gas phase with a liquid that is immiscible with the reagents. Moreover, working with all-liquid systems allows production of, instead of slugs, droplets that are completely surrounded by the immiscible continuous phase. Additionally, droplets are usually smaller than slugs, thereby benefiting even more from the advantages of miniaturized synthesis.

In recent years, the synthesis of nanoparticles in microfluidic devices has attracted much attention, and different types of nanometre-sized materials have been produced on-chip,[6,7,9–11] for example metals,[12–14] quantum dots,[12,15] organic polymers[16,17] and metal oxides.[8,12,18] Due to the steady-flow regime in which these devices can operate, the reaction products can be continuously evaluated, and reaction conditions constantly adjusted.[12] Furthermore, the form factor of microfluidic chips entails a massive increase in the surface-to-volume ratio, leading to an enhanced heat and mass transfer[10] and a higher reaction efficiency.[7] Two different types of hydrodynamic conditions have been utilized to synthesize nanoparticles in microfluidic devices: continuous flow reactors, where the reagents are injected into a single channel and mixed (often solely *via* diffusion),[13,15,16,18–20] and segmented flow patterns, where the flow containing the reagents is compartmentalized, and where compartments are separated by a spacer consisting of an immiscible phase.[8,12–14,17] While devices based on the continuous flow regime are more controllable, they often produce nanoparticles with relatively large size distributions, due to the Taylor–Aris dispersion originating from the parabolic flow profile in the microchannels.[21] In a segmented flow pattern, reaction volumes are very well controlled and the liquids can

Laboratory of Microsystems, Ecole Polytechnique Fédérale de Lausanne, 1015 Lausanne, Switzerland. E-mail: josias.wacker@epfl.ch; Fax: +41 21 693 77 31; Tel: +41 21 693 65 84

† Electronic Supplementary Information (ESI) available: Scheme of the experimental setup for the photochemical bleaching experiment, microscope image showing mixing inside droplets, calculative estimation of nanoparticle production. See DOI: 10.1039/c2lc40300e

moreover circulate inside the compartments, resulting in a more homogeneous mixing of reagents, a more uniform particle synthesis time and thus a narrower particle size distribution.[21]

The final size of synthesized nanoparticles strongly depends on the relative concentrations of the different reagents. Inside microfluidic droplets, these concentrations can be easily adjusted by changing the rate at which the reagent streams are fed into the chip. A second parameter that influences the size of the nanoparticles, the reaction time, can be controlled by adjusting the on-chip residence time by varying the flow rate of the liquids and the length of the microchannels. While the importance of reaction time has been elucidated for several types of nanoparticle,[12,22,23] the influence of reagent flow rates has been studied for only a few kinds of nanoparticle (see *e.g.* ref. 24).

For several applications (*e.g.* biological cell studies), it is desirable that the synthesized nanoparticles are detectable with high contrast using an optical microscope. To this end, the controlled synthesis of fluorescent quantum dots in microfluidic droplets and slugs has been widely studied.[9,25] However, most quantum dots contain heavy metals, which are potentially hazardous to health and may cause cell-death in biological experiments.[26] Silica nanoparticles, on the other hand, are chemically inert in a cellular environment and therefore less likely to interfere in an undesired way with a biological sample.[27] However, to the best of our knowledge, microsynthesis of fluorescent silica nanoparticles has only been shown in continuous flow reactors.[19] Unfortunately, the influence of the reaction time and of the reagent concentrations on the morphology of the particles is missing in this preliminary study, and therefore only particles with 50 nm diameters are reported.

Here, we present how microdroplet-based synthesis permits fine-tuning of the size of silica nanoparticles *via* two parameters, namely the reaction time and the concentration of reagents. In addition, we incorporated a fluorescent dye into the nanoparticles, thus demonstrating the first chip-based synthesis of fluorescently functionalized silica nanoparticles of a wide range of sizes in droplets.

Materials and methods

Microdroplet-based synthesis of fluorescent silica nanoparticles

Unless stated differently, chemicals were purchased from Sigma Aldrich, Buchs, Switzerland. Microfluidic chips were made of polydimethyl siloxane (PDMS Sylgard 184, from Dow Corning) using soft lithography.[28] In short, PDMS was mixed with a polymerizing catalyst, poured over an SU-8 mould that defined the channel geometry, and cured at 60 °C overnight. All channels were 40 μm in height; the oil inlet channels were 400 μm wide and the inlet channels for the silicon alkoxide solution (SA) and the hydrolysing mixture (HM) were 100 μm in width. The outlet channel was 300 μm wide and 230 mm long. After curing of the PDMS, the chips were plasma-bonded to glass slides that had been coated with PDMS. To make the channels hydrophobic, they were rinsed for 1 min with Aquapel (Pittsburgh Glass Works, Pennsylvania, USA), a commercially available fluorinated glass hydrophobiser, and dried at 50 °C for 30 min. HM was prepared by mixing 4 mL dry ethanol with 2 mL aqueous ammonia (29%) and 90 μL de-ionized water. To prepare the SA, 0.69 g APTES was dissolved in 6.9 mL dry ethanol, and mixed with 5.3 mg FITC during 20 h under exclusion of light and moisture. 250 μL of this fluorescent solution was then added to 4 mL dry ethanol and 250 μL TEOS. Using glass syringes (ILS, Stützerbach, Germany) and syringe pumps (neMESYS, Cetoni, Korbussen, Germany), HM, SA and FC-40 Fluorinert oil were injected separately into the microfluidic chips, typically at flow rates of 0.5 μL s^{-1} (FC-40), 0.003 μL s^{-1} (SA) and 0.003 μL s^{-1} or 0.006 μL s^{-1} (HM). High flow rates are required to avoid pinning of the droplets to the channel walls. After passing through the outlet tubing, the liquids were collected on silicon dies and immediately evaporated at 200 °C. Microscope movies of droplets were taken at ~1000 frames per second with a high-speed camera (GMCTLTR1 from Mikrotron, Unterschleissheim, Germany).

Batch synthesis of fluorescent silica nanoparticles

Batch synthesis of nanoparticles was done by mixing 1 mL SA with 1 mL HM (HM : SA = 1 : 1) or 1.5 mL HM with 0.75 mL SA (HM : SA = 2 : 1) in a 15 mL glass vial under stirring (300 rpm). APTES-free nanoparticles were synthesized by diluting 0.69 mL TEOS in 6.9 mL ethanol and mixing with 5.3 mg FITC for 20 h. The APTES-free fluorescent solution is then used like the APTES–FITC solution described previously.

Microscopic inspection of fluorescent silica nanoparticles

All particles were optically analysed using an upright microscope (Axio Imager from Zeiss and Eclipse E600 from Nikon) with an appropriate filter setup (FS 10 from Zeiss and FITC from Nikon). Images were taken using a CCD camera (Hamamatsu, Japan and Zeiss, Germany). SEM images were taken with a XLF-30-FEG microscope, TEM images with a FEI CM12 microscope.

Bleaching experiments

For the bleaching experiments, rectangular capillaries (300 μm wide) were filled with an aqueous suspension of dye-labelled nanoparticles (7 min reaction time, HM : SA = 2 : 1) or FITC (0.1 mg mL^{-1} in water) and sealed with FC-40. For each experiment, two capillaries were prepared, one containing ~50 nL fluorescent solution and one serving as a reference (containing ~500 nL fluorescent solution). The capillary with less solution was permanently exposed to the light (450–490 nm wavelength) originating from a mercury arc lamp (50 W), while the reference solution was protected from light (a scheme of the experimental setup is given in the ESI†). Every 30 s, a fluorescence photograph was taken of both capillaries (exposure time: ~500 ms). Bleaching analysis was done by normalizing the mean background-corrected brightness (we subtracted the background intensity from the signal) of the bleached solution with the mean background-corrected reference solution. Bleaching curves were then obtained by dividing the normalized mean values by the normalized background-corrected mean value of the unexposed sample.

Results and discussion

To synthesize fluorescent silica nanoparticles in microdroplets, we adapted the protocol developed by Stöber *et al.*[29] The

synthesis involves hydrolysis of TEOS, which is catalysed by aqueous ammonia (NH_4OH), as follows:

$$\equiv Si–OC_2H_5 + H_2O \rightarrow \equiv Si–OH + C_2H_5OH \quad (1)$$

Nanoparticle formation proceeds *via* two condensation reactions:

$$\equiv Si–OH + HO–Si\equiv \rightarrow \equiv Si–O–Si\equiv + H_2O \quad (2)$$

$$\equiv Si–OC_2H_5 + HO–Si\equiv \rightarrow \equiv Si–O–Si + C_2H_5OH \quad (3)$$

To produce fluorescent silica nanoparticles, we used a low amount of APTES to bind FITC to the silica network *via* thiourea-linkages.[19,30] Fig. 1 shows schematically the whole synthesis procedure. APTES and FITC were mixed off-chip in dry ethanol during 20 h under the exclusion of light. We then added TEOS to the alcoholic solution of fluorescent APTES and injected this SA into the droplet-producing microfluidic chip. An alcoholic HM containing NH_4OH and water entered the chip *via* a second inlet and merged with the fluorescent SA. This stream, containing all reagents, was transformed into droplets at a flow-focusing junction, where a flow of FC-40 pinched it off. Since a homogeneous distribution of the reagents throughout the reaction vessel (droplet) is indispensable for obtaining monodisperse nanoparticles, others[8] designed channels to induce mixing between the SA and the HM before droplet formation, while our meandering channel ensures reagent mixing after droplet formation. We studied this type of mixing by observing half coloured/half transparent droplets, and found that the colour gradient between the halves dramatically decreased after only two U-turns ($\sim$0.1 s) of the meandering outlet channel (see ESI†). Therefore, we waived pre-mixing structures in our chip.

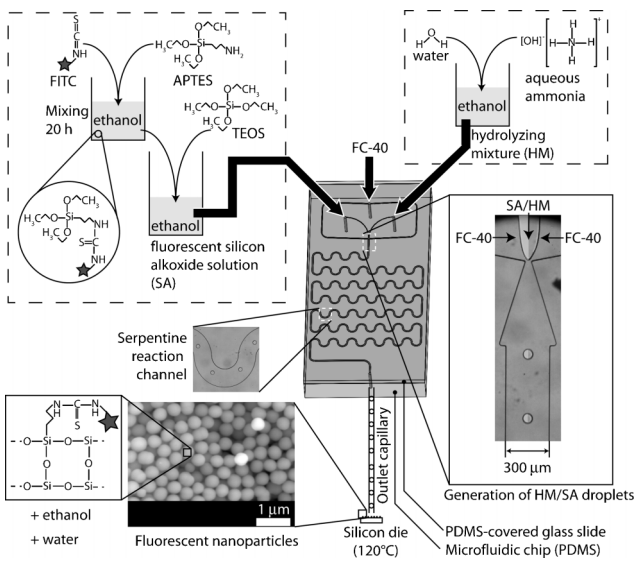

Fig. 1 Procedure and setup for the droplet-based synthesis of fluorescent SiO_2 nanoparticles. FITC is coupled to APTES and mixed off-chip with TEOS to yield a fluorescent silicon alkoxide solution (SA). A hydrolysing mixture (HM) and SA are injected into the microfluidic chip, where they are merged and converted into a stream of droplets in Fluorinert oil (FC-40) by a flow-focusing nozzle. After evaporation of the reagents, the SiO_2 nanoparticles are analysed by electron microscopy.

To stabilize the droplets, we added 0.125% v/v fluorinated surfactant (Zonyl FSO) to the FC-40. After passing through a meandering reaction channel on the chip and an outlet capillary, the droplets, together with the oil, were deposited on a heated silicon die by slightly touching the latter with the outlet capillary. The liquids immediately evaporated, quenching the synthesis reaction. This way, nanoparticles formed in the droplets were extracted from the chip and out of the droplet phase and collected on the silicon die.

To change the concentrations of reagents inside the droplets, we varied the relative volumetric flow rates of SA and HM to HM : SA = 1 : 1 and 2 : 1. Table 1 shows the molarities of the reagents inside the droplets for the respective flow conditions. We estimate that the production rate of nanoparticles is between 60×10^6 min^{-1} and 90×10^6 min^{-1}, for the used reaction conditions (see ESI†). The production yield can, however, be easily up-scaled by parallelization of the microfluidic device.[31]

As shown by the curves in Fig. 2(a), longer reaction times and bigger content of HM in each droplet yield bigger nanoparticles. The reaction time dependence is in good accordance with previous studies[8,22] and is explained by the progressive continuous growth process of the SiO_2 nanoparticles. The influence of reagent molarities is more pronounced at short reaction times. From previous bulk-reaction studies, it is known that the hydrolysis reaction (1) is the slowest step in nanoparticle synthesis.[32] As suggested by Bogush and Zukoski, hydrolysis and condensation of a few molecules initiate the formation of nuclei, and particle growth proceeds *via* agglomeration of these nuclei.[33] A shift towards a higher molarity of NH_4OH accelerates hydrolysis and the formation of nuclei, and a higher water concentration favours the agglomeration of these nuclei due to a higher availability of hydrogen bonds on the surface of existing nanoparticles.[34] Therefore, the influence of NH_4OH and water is more pronounced in the early stages of nanoparticle formation than at longer reaction times, when the nuclei were given time to form and agglomerate, independent of the molarities of the reagents. The tight size controllability of the proposed method is also reflected by the good monodispersity of the particles, as evidenced in Fig. 2(a) by the low coefficients of variance (CV = σ/μ, where μ is the mean diameter of the particles and σ the standard deviation, as obtained from analysis of scanning electron microscopy (SEM) graphs). Our functionalized, on-chip synthesized nanoparticles are approximately as monodisperse as non-functionalized nanoparticles that are obtained from traditional synthesis in bulk (see *e.g.* ref. 35). The uniformity of the size and shape of the on-chip synthesised nanoparticles was further confirmed by transmission electron microscopy (TEM), see Fig. 2(b). Additional analysis with high-resolution TEM indicates a morphology of the nanoparticles

Table 1 Molarities of reactants under different flow conditions

	Relative flow rates (HM : SA)	
Reagents	1 : 1	2 : 1
Water	6.25 M	8.3 M
NH_4OH	1.2 M	1.6 M
TEOS	0.13 M	0.083 M
APTES	0.012 M	0.008 M
Ethanol	13.28 M	12.6 M

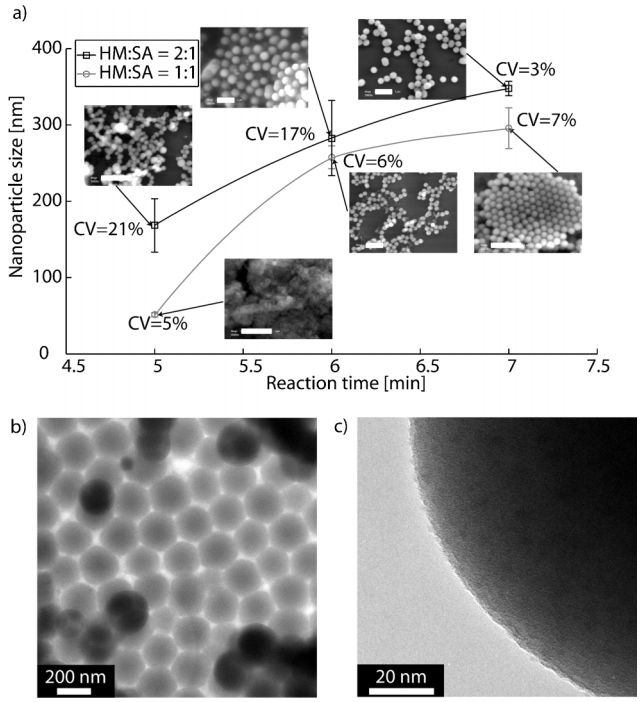

Fig. 2 (a) Size of the on-chip synthesized SiO_2 nanoparticles as a function of reaction time with the reagent concentration ratio HM : SA as a parameter. The size distributions of the nanoparticles are given as coefficients of variance (CV). The scale bars in the inset scanning electron microscopy (SEM) graphs are 1 μm. (b and c) Transmission electron microscopy (TEM) graphs of on-chip synthesized fluorescent SiO_2 nanoparticles.

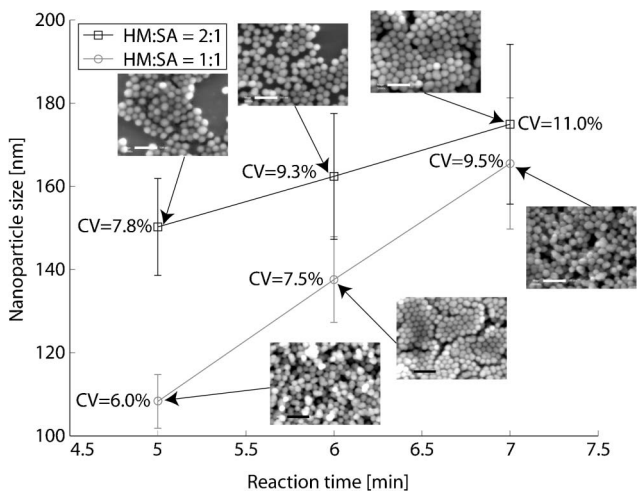

Fig. 3 Size of the bulk-synthesized SiO_2 nanoparticles as a function of reaction time with the reagent concentration ratio HM : SA as a parameter. The scale bars in the SEM insets are 500 nm. In bulk, particle growth is slower than in droplets.

characterized by a low surface roughness and no apparent pores at the surface (see Fig. 2(c)).

We found qualitatively similar results in the bulk synthesis of fluorescent SiO_2 nanoparticles (see Fig. 3). Remarkably, the growth rate at the later stages is slower in bulk synthesis than in droplet-based synthesis, resulting in smaller particles for the longer reaction times. We think that this is due to the more vigorous mixing in the bulk synthesis process using a magnetic stirrer, which leads to the formation of more nuclei on which silica precursor species adhere, leading to a larger number of smaller nanoparticles. The growth rate of particles is controlled by diffusive processes and shows a saturating behaviour at longer reaction times for the on-chip synthesis, as shown in Fig. 2(a). We think this can be explained by the consumption of all precursor materials present within a droplet, while such saturating behaviour is not expected on this timescale in bulk synthesis. In addition, strong stirring may disintegrate growing particles. We also noted that, in the microfluidic chip, HM and SA flow in parallel before forming droplets and that TEOS molecules at the interface between the two streams may undergo hydrolysis prior to molecules which are further away from the interface. These molecules may serve as pre-nuclei, which then grow by deposition of subsequently formed nuclei.

Applications of silica nanoparticles do not only rely on the precise control of their size and size distribution, but also on any type of additional functionality they may have.[1,3,36] To show the suitability of droplet microfluidics for the synthesis of functionalized nanoparticles, we embedded the organic dye FITC in our SiO_2 nanoparticles and studied the fluorescent properties of the latter. The photographs in Fig. 4(a) and 4(b) are taken with an optical microscope and show the fluorescent characteristics of the particles. Fig. 4(a) shows a bright field (no filter) and a fluorescent (FITC emission/excitation filter) image of the same sample and proves that the particles can be functionalized by incorporation of FITC. To verify that the fluorescent dye did not leak out of the particles, we washed the nanoparticle samples 10 times with ethanol and inspected them with a fluorescent microscope after each washing step. Fig. 4(b) shows fluorescent micrographs of nanoparticles prepared with either our APTES-based or an APTES-free protocol before the washing procedure and after the tenth washing cycle. In each washing cycle, we applied, in a Teflon beaker, a gently agitated flow of ethanol during 2 min to the silicon die carrying the nanoparticles. After removing the silicon die from the beaker, the remaining ethanol was evaporated at room temperature. When the nanoparticles were synthesized using the APTES-based process, the mean intensity of the fluorescent image was basically identical before and after 10 washing cycles, confirming that the dye was well embedded in the particles. However, nanoparticles prepared using an APTES-free protocol were only weakly fluorescent after 10 washing cycles ($\sim$2 times lower mean intensity), indicating a progressive loss of dye.

Fluorescent dyes generally lose their brightness while being illuminated (so-called photobleaching). For long-term studies, it is important that the dye remains stable during extended illumination periods. It has been shown that embedding fluorescent dyes in silica nanoparticles reduces photobleaching.[37,38] We compared the photochemical bleaching of on-chip synthesised fluorescent SiO_2 nanoparticles with pure FITC. The curves in Fig. 4(c) show the decrease of fluorescence intensity for the two samples under continuous illumination with a mercury lamp. As shown by the bleaching curves, the fluorescent SiO_2 nanoparticles bleach more slowly than pure FITC in de-ionized water.

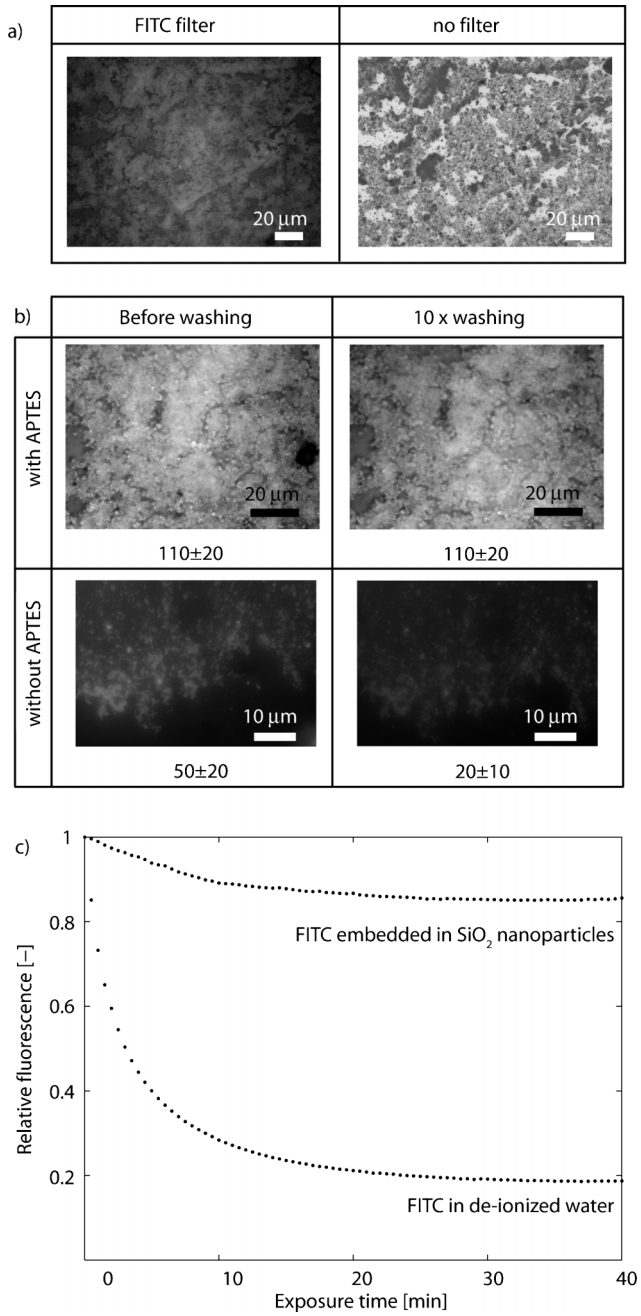

Fig. 4 Analysis of the fluorescent properties of the nanoparticles. (a) Nanoparticles viewed through a FITC filter and in bright field (no filter). (b) Nanoparticles prepared using an APTES-based and an APTES-free protocol before and after applying 10 washing cycles in ethanol, showing that FITC is not leaking out of the nanoparticles prepared with the APTES-based protocol. The numbers indicate the mean and the single standard deviation of the grey values in the microscopy photographs. (c) Comparison of the bleaching behaviour between FITC that is incorporated in SiO_2 nanoparticles (7 min reaction time, HM : SA = 2 : 1, suspended in de-ionized water) and free FITC in de-ionized water, showing faster photochemical bleaching of the pure dye.

Conclusions

In the present study we have shown how droplet microfluidics permits the controlled synthesis of functionalized nanoparticles. We presented two different strategies to tune the size of the nanoparticles: adjustment of the reaction time and of reagent concentrations. We compared droplet-based synthesis with conventional bulk-synthesis and found that the nanoparticle growth speed is higher for droplet-based synthesis, and therefore the size of the nanoparticles can be controlled over a wider range in a shorter time. We functionalized the nanoparticles with FITC fluorescent dye and found that they photobleach more slowly than when the dye is used free in solution. APTES, the linker molecule between the SiO_2 network and the organic dye, can be derivatized with a wide family of molecules, including biomolecules, thus opening perspectives for the microdroplet-based synthesis of nanoparticles with multiple functionalities. In the light of the relatively low production rate and the high degree of size controllability, the presented microfluidic nanoparticle synthesis method is especially suitable for the integrated production and use of well-controlled small aliquots of nanoparticles, *e.g.* for diagnostic lab-on-a-chip applications.

Acknowledgements

The authors acknowledge the Swiss National Science Foundation for financial support (Grant No.137577).

References

1 I. I. Slowing, J. L. Vivero-Escoto, C. W. Wu and V. S. Y. Lin, *Adv. Drug Delivery Rev.*, 2008, **60**, 1278–1288.
2 A. N. Shipway, E. Katz and I. Willner, *ChemPhysChem*, 2000, **1**, 18–52.
3 A. Burns, H. Ow and U. Wiesner, *Chem. Soc. Rev.*, 2006, **35**, 1028–1042.
4 O. D. Velev and K. H. Bhatt, *Soft Matter*, 2006, **2**, 738–750.
5 M. A. M. Gijs, F. Lacharme and U. Lehmann, *Chem. Rev.*, 2010, **110**, 1518–1563.
6 M. Pumera, *Chem. Commun.*, 2011, **47**, 5671–5680.
7 S. Marre and K. F. Jensen, *Chem. Soc. Rev.*, 2010, **39**, 1183–1202.
8 S. A. Khan, A. Günther, M. A. Schmidt and K. F. Jensen, *Langmuir*, 2004, **20**, 8604–8611.
9 T. J. Wang, J. Wang and J.-J. Han, *Small*, 2011, **7**, 1728–1754.
10 A. Abou-Hassan, O. Sandre and V. Cabuil, *Angew. Chem., Int. Ed.*, 2010, **49**, 6268–6286.
11 J. B. Wacker, V. K. Parashar and M. A. M. Gijs, *RSC Adv.*, 2012, **2**, 3599–3601.
12 A. M. Nightingale, S. H. Krishnadasan, D. Berhanu, X. Niu, C. Drury, R. Mcintyre, E. Valsami-Jones and J. C. Demello, *Lab Chip*, 2011, **11**, 1221–1227.
13 L. L. Lazarus, A. S. J. Yang, S. Chu, R. L. Brutchey and N. Malmstadt, *Lab Chip*, 2010, **10**, 3377–3379.
14 S. Duraiswamy and S. A. Khan, *Small*, 2009, **5**, 2828–2834.
15 S. Krishnadasan, R. J. C. Brown, A. J. Demello and J. C. Demello, *Lab Chip*, 2007, **7**, 1434–1441.
16 M. Rhee, P. M. Valencia, M. I. Rodriguez, R. Langer, O. C. Farokhzad and R. Karnik, *Adv. Mater.*, 2011, **23**, H79–H83.
17 K. Liu, H. Wang, K. J. Chen, F. Guo, W. Y. Lin, Y. C. Chen, D. L. Phung, H. R. Tseng and C. K. F. Shen, *Nanotechnology*, 2010, **21**, 8.
18 C. K. Chung, T. R. Shih, C. K. Chang, C. W. Lai and B. H. Wu, *Chem. Eng. J.*, 2011, **168**, 790–798.
19 A. Abou-Hassan, R. Bazzi and V. Cabuil, *Angew. Chem., Int. Ed.*, 2009, **48**, 7180–7183.
20 V. Genot, S. Desportes, C. Croushore, J. P. Lefevre, R. B. Pansu, J. A. Delaire and P. R. Von Rohr, *Chem. Eng. J.*, 2010, **161**, 234–239.
21 A. Huebner, S. Sharma, M. Srisa-Art, F. Hollfelder, J. B. Edel and A. J. Demello, *Lab Chip*, 2008, **8**, 1244–1254.
22 A. Günther, S. A. Khan, M. Thalmann, F. Trachsel and K. F. Jensen, *Lab Chip*, 2004, **4**, 278–286.
23 Z. Wan, H. W. Yang, W. L. Luan, S. T. Tu and X. G. Zhou, *Nanoscale Res. Lett.*, 2010, **5**, 130–137.
24 S. Li, J. Xu, Y. Wang and G. Luo, *Langmuir*, 2008, **24**, 4194–4199.

25 A. M. Nightingale and J. C. J. De Mello, *J. Mater. Chem.*, 2010, **20**, 8454–8463.
26 A. M. Derfus, W. C. W. Chan and S. N. Bhatia, *Nano Lett.*, 2004, **4**, 11–18.
27 T. J. Brunner, P. Wick, P. Manser, P. Spohn, R. N. Grass, L. K. Limbach, A. Bruinink and W. J. Stark, *Environ. Sci. Technol.*, 2006, **40**, 4374–4381.
28 Y. Xia and G. M. Whitesides, *Angew. Chem., Int. Ed.*, 1998, **37**, 550–575.
29 W. Stöber, A. Fink and E. J. Bohn, *J. Colloid Interface Sci.*, 1968, **26**, 62–69.
30 A. Vanblaaderen and A. Vrij, *Langmuir*, 1992, **8**, 2921–2931.
31 T. Nisisako and T. Torii, *Lab Chip*, 2008, **8**, 287–293.
32 S. K. Park, K. D. Kim and H. T. Kim, *Colloids Surf., A*, 2002, **197**, 7–17.
33 G. H. Bogush and C. F. J. Zukoski IV, *J. Colloid Interface Sci.*, 1991, **142**, 1–18.
34 K. S. Rao, K. El-Hami, T. Kodaki, K. Matsushige and K. J. Makino, *J. Colloid Interface Sci.*, 2005, **289**, 125–131.
35 N. Plumeré, A. Ruff, B. Speiser, V. Feldmann and H. A. J. Mayer, *J. Colloid Interface Sci.*, 2012, **368**, 208–219.
36 D. Knopp, D. P. Tang and R. Niessner, *Anal. Chim. Acta*, 2009, **647**, 14–30.
37 M. Nakamura, M. Shono and K. Ishimura, *Anal. Chem.*, 2007, **79**, 6507–6514.
38 H. Ow, D. R. Larson, M. Srivastava, B. A. Baird, W. W. Webb and U. Wiesner, *Nano Lett.*, 2004, **5**, 113–117.

